

Supporting Information

# Efficient photocatalytic CO<sub>2</sub> reduction with MIL-100(Fe)-CsPbBr<sub>3</sub> composites

Ruolin Cheng<sup>1</sup>, Elke Debroye<sup>1</sup>, Johan Hofkens<sup>1,\*</sup> and Maarten B.J. Roeffaers<sup>2,\*</sup>

<sup>1</sup> Department of Chemistry, Faculty of Sciences, KU Leuven, Celestijnenlaan 200F, 3001 Leuven, Belgium

<sup>2</sup> Center for membrane separations, adsorption, catalysis and spectroscopy for sustainable solutions (cMACS), KU Leuven, Celestijnenlaan 200F, 3001 Leuven, Belgium

\* Correspondence: johan.hofkens@kuleuven.be (J.H.) maarten.roeffaers@kuleuven.be (M.B.J.R.)

## Supplementary Figures and Tables

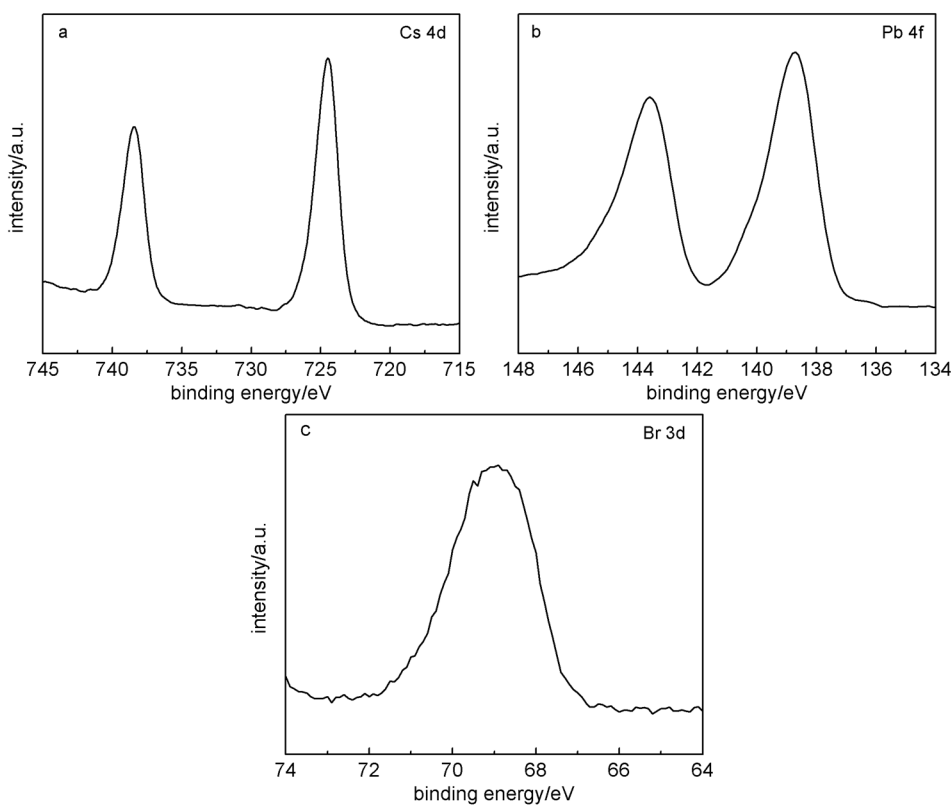


**Figure S1.** XPS spectra of p-90Fe: (a) Cs 3d, (b) Pb 4f and (c) Br 3d.

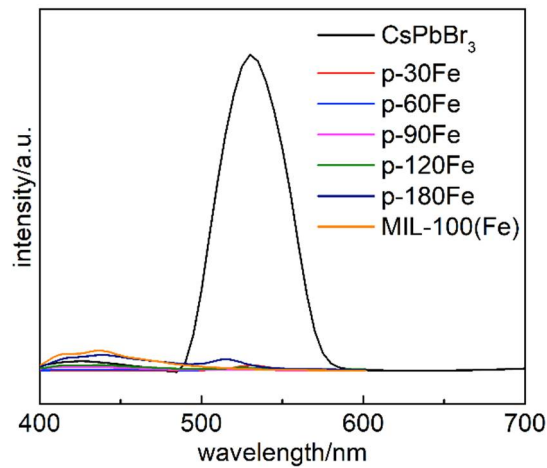


**Figure S2.** Photoluminescence spectra of the as-prepared samples at an excitation wavelength of 380 nm.

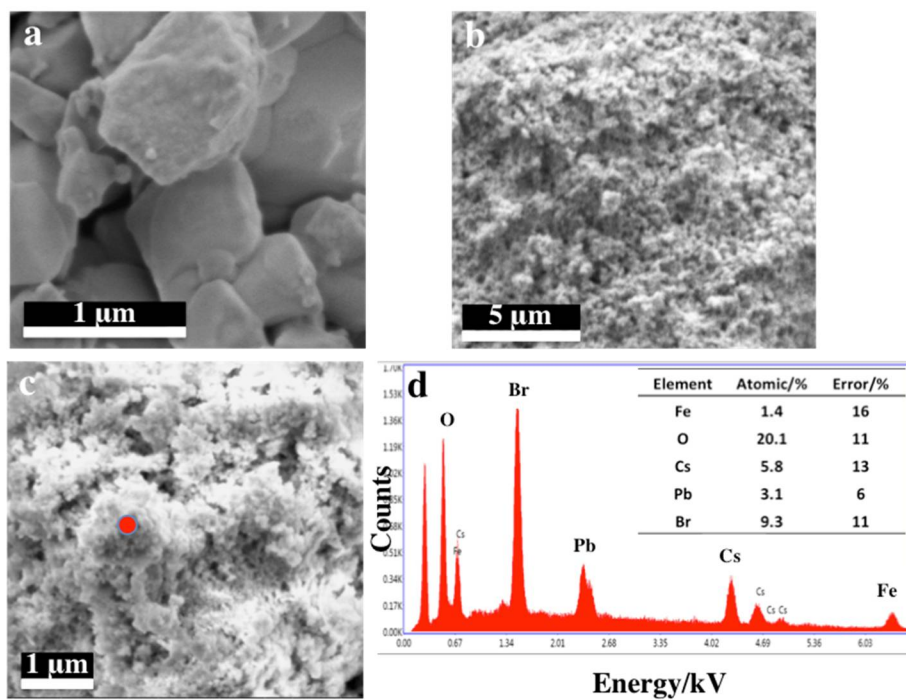


**Figure S3.** Typical SEM images of (a) CsPbBr<sub>3</sub>, (b) MIL-100(Fe), (c) p-90Fe and (d) EDS pattern of the selected region in (c) p-90Fe.

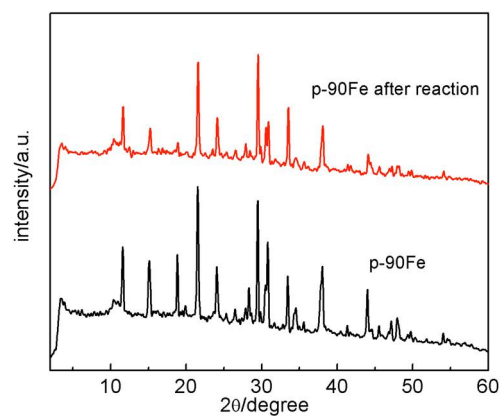


**Figure S4.** XRD pattern of p-90Fe before and after a 16 h photocatalytic reaction.**Table S1.** Summary of the reported photocatalytic CO<sub>2</sub> reduction performance of perovskite-based and traditional photocatalysts under various illumination conditions.

Catalyst	System	Light source	Major product	R <sub>electrons</sub> (μmol/g/h)	Ref
CsPbBr <sub>3</sub>	H <sub>2</sub> O vapor	300 W Xe lamp visible light (>420 nm)	CO	9	This work
MIL-100(Fe)				10	
CsPbBr <sub>3</sub> /MIL-100(Fe)				41	
CsPbBr <sub>3</sub> /MIL-100(Fe)		300 W Xe lamp full spectrum		59	
CsPbBr <sub>3</sub> QD	H <sub>2</sub> O vapor	100 W Xe lamp AM 1.5G	CH <sub>4</sub> (minor CO)	11	[1]
ZIF-8				2	
ZIF-67				4	
CsPbBr <sub>3</sub> /ZIF-8				15	
CsPbBr <sub>3</sub> /ZIF-67				30	
CsPbBr <sub>3</sub> QD	ethyl acetate	100 W Xe lamp AM 1.5G	CO (minor CH <sub>4</sub> )	24	[2]
CsPbBr <sub>3</sub> QD/GO				30	
CsPbBr <sub>3</sub> QD/ UiO-66-NH <sub>2</sub>	H <sub>2</sub> O/ethyl acetate	300 W Xe lamp visible light (>420 nm)	CO (trace CH <sub>4</sub> )	19	[3]
UiO-66-NH <sub>2</sub>				1	
UiO-66-NH <sub>2</sub>	CO <sub>2</sub> /H <sub>2</sub>	150 W Xe lamp, λ > 325 nm	CO	3	[4]
g-C <sub>3</sub> N <sub>4</sub>	H <sub>2</sub> O vapor	300 W Xe lamp visible light (>420 nm)	CO	14	[5]
Bi <sub>2</sub> WO <sub>6</sub> /g-C <sub>3</sub> N <sub>4</sub>	H <sub>2</sub> O vapor	300 W Xe lamp visible light (>420 nm)	CO	10	[6]
bulk g-C <sub>3</sub> N <sub>4</sub>	MeCN/TEOA	300 W Xe lamp visible light (>400 nm)	CO	4	[7]
g-C <sub>3</sub> N <sub>4</sub> nanosheets				6	
UiO-66				0	
UiO-66/g-C <sub>3</sub> N <sub>4</sub> nanosheets				20	
anatase TiO <sub>2</sub>				H <sub>2</sub> O vapor	
anatase TiO <sub>2</sub>	H <sub>2</sub> O vapor	300 W Xe lamp full spectrum	CO	8	[9]
ZIF-L				1	
TiO <sub>2</sub> /C@ZnCo-ZIF-L				57	
Cu-BTC	H <sub>2</sub> O vapor	300 W Xe lamp UV(<400 nm)	CH <sub>4</sub>	0	[10]
Cu-BTC/TiO <sub>2</sub>				8	
WO <sub>3</sub>	H <sub>2</sub> O	300 W Xe lamp visible light (>420 nm)	CH <sub>4</sub>	9	[11]
MIL-125(Ti)-NH <sub>2</sub>	H <sub>2</sub> O vapor	300 W Xe lamp visible light (>420 nm)	CH <sub>4</sub>	3	[12]
MIL-101(Fe)	MeCN/TEOA	300 W Xe lamp visible light (>420 nm)	HCOO <sup>-</sup>	294	[13]
MIL-101(Fe)-NH <sub>2</sub>				890	
MIL-53(Fe)				148.4	
MIL-53(Fe)-NH <sub>2</sub>				232.4	
MIL-88B(Fe)				45	
MIL-88B(Fe)-NH <sub>2</sub>				150	

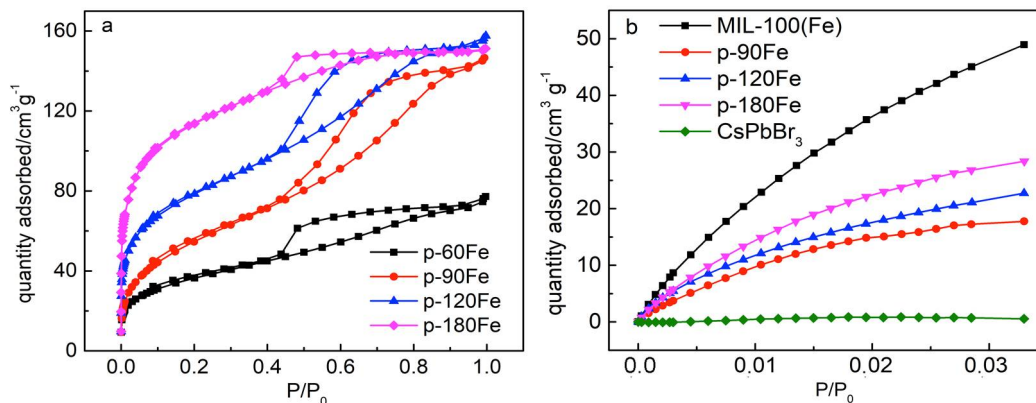


**Figure S5.** (a) N<sub>2</sub> adsorption-desorption isotherms and (b) CO<sub>2</sub> adsorption isotherms of the photocatalysts.

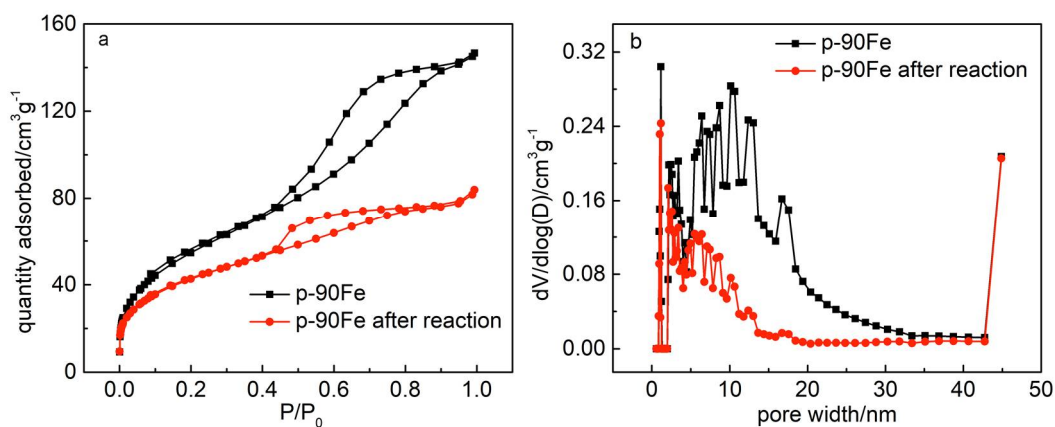


**Figure S6.** (a) N<sub>2</sub> adsorption-desorption isotherms and (b) pore size distribution curves of the p-90Fe before and after reaction.

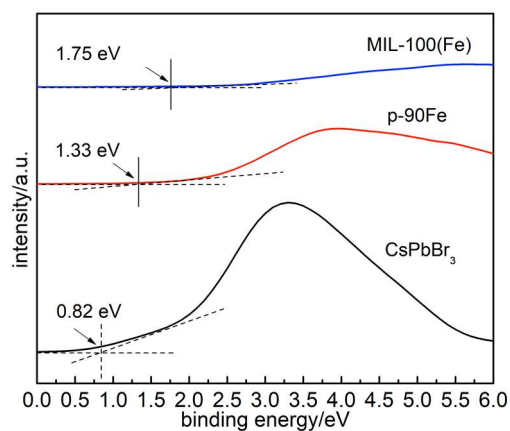


**Figure S7.** Valence band XPS spectra of MIL-100(Fe), CsPbBr<sub>3</sub> and p-90Fe.

## References

1. Kong, Z. C.; Liao, J. F.; Dong, Y. J.; Xu, Y. F.; Chen, H. Y.; Kuang, D. B.; Su, C. Y. Core@Shell CsPbBr<sub>3</sub>@Zeolitic Imidazolate Framework Nanocomposite for Efficient Photocatalytic CO<sub>2</sub> Reduction. *Acs Energy Lett.* **2018**, *3* (11), 2656-2662.
2. Xu, Y. F.; Yang, M. Z.; Chen, B. X.; Wang, X. D.; Chen, H. Y.; Kuang, D. B.; Su, C. Y. A CsPbBr<sub>3</sub> Perovskite Quantum Dot/Graphene Oxide Composite for Photocatalytic CO<sub>2</sub> Reduction. *J. Am. Chem. Soc.* **2017**, *139*, 5660-5663.
3. Wan, S. P.; Ou, M.; Zhong, Q.; Wang, X. M. Perovskite-type CsPbBr<sub>3</sub> quantum dots/Uio-66(NH<sub>2</sub>) nanojunction as efficient visible-light-driven photocatalyst for CO<sub>2</sub> reduction. *Chem. Eng. J.* **2019**, *358*, 1287-1295.
4. Crake, A.; Christoforidis, K. C.; Kafizas, A.; Zafeirotos, S.; Petit, C. CO<sub>2</sub> capture and photocatalytic reduction using bifunctional TiO<sub>2</sub>/MOF nanocomposites under UV-vis irradiation. *Appl. Catal., B* **2017**, *210*, 131-140.
5. Liu, C.; Zhang, Y.; Dong, F.; Reshak, A. H.; Ye, L.; Pinna, N.; Zeng, C.; Zhang, T.; Huang, H. Chlorine intercalation in graphitic carbon nitride for efficient photocatalysis. *Appl. Catal., B* **2017**, *203*, 465-474.
6. Li, M.; Zhang, L.; Fan, X.; Zhou, Y.; Wu, M.; Shi, J. Highly selective CO<sub>2</sub> photoreduction to CO over g-C<sub>3</sub>N<sub>4</sub>/Bi<sub>2</sub>WO<sub>6</sub> composites under visible light. *J. Mater. Chem. A* **2015**, *3* (9), 5189-5196.
7. Shi, L.; Wang, T.; Zhang, H. B.; Chang, K.; Ye, J. H. Electrostatic Self-Assembly of Nanosized Carbon Nitride Nanosheet onto a Zirconium Metal-Organic Framework for Enhanced Photocatalytic CO<sub>2</sub> Reduction. *Adv. Funct. Mater.* **2015**, *25* (33), 5360-5367.
8. Zhao, Y. L.; Wei, Y. C.; Wu, X. X.; Zheng, H. L.; Zhao, Z.; Liu, J.; Li, J. M. Graphene-wrapped Pt/TiO<sub>2</sub> photocatalysts with enhanced photogenerated charges separation and reactant adsorption for high selective photoreduction of CO<sub>2</sub> to CH<sub>4</sub>. *Appl. Catal., B* **2018**, *226*, 360-372.
9. Zhou, A. W.; Dou, Y. B.; Zhao, C.; Zhou, J.; Wu, X. Q.; Li, J. R. A leaf-branch TiO<sub>2</sub>/carbon@MOF composite for selective CO<sub>2</sub> photoreduction. *Appl. Catal., B* **2020**, *264*, 118519-118526.
10. Li, R.; Hu, J. H.; Deng, M. S.; Wang, H. L.; Wang, X. J.; Hu, Y. L.; Jiang, H. L.; Jiang, J.; Zhang, Q.; Xie, Y.; Xiong, Y. J. Integration of an Inorganic Semiconductor with a Metal-Organic Framework: A Platform for Enhanced Gaseous Photocatalytic Reactions. *Adv. Mater.* **2014**, *26* (28), 4783-4788.
11. Chen, X. Y.; Zhou, Y.; Liu, Q.; Li, Z. D.; Liu, J. G.; Zou, Z. G. Ultrathin, Single-Crystal WO<sub>3</sub> Nanosheets by Two-Dimensional Oriented Attachment toward Enhanced Photocatalytic Reduction of CO<sub>2</sub> into Hydrocarbon Fuels under Visible Light. *Acs Appl. Mater. Inter.* **2012**, *4* (7), 3372-3377.
12. Hu, J. M.; Ding, J.; Zhong, Q. In situ fabrication of amorphous TiO<sub>2</sub>/NH<sub>2</sub>-MIL-125(Ti) for enhanced photocatalytic CO<sub>2</sub> into CH<sub>4</sub> with H<sub>2</sub>O under visible-light irradiation. *J. Colloid Interf. Sci.* **2020**, *560*, 857-865.
13. Wang, D. K.; Huang, R. K.; Liu, W. J.; Sun, D. R.; Li, Z. H. Fe-Based MOFs for Photocatalytic CO<sub>2</sub> Reduction: Role of Coordination Unsaturated Sites and Dual Excitation Pathways. *Acs Catal.* **2014**, *4* (12), 4254-4260.

